Electronic Supporting Information

In Situ Supramolecular Self-assembly of Perylene Diimide Derivative in Mitochondria for Cancer Cell Ferroptosis

Xuan Wu,[a*] Ling-Long Zhuang,[c] Ming Liu,[d] Xiaohuan Sun,[a] Liqi Zhu,[c] Quan Zhang,[c] Jie Han,[a*] Leyong Wang,[b] Rong Guo[a]

[a] School of Chemistry and Chemical Engineering, Yangzhou University, Yangzhou 225002, China

[b] School of Chemistry and Chemical Engineering, Nanjing University, Nanjing, 210023.

[c] College of Veterinary Medicine, Yangzhou University, Yangzhou 225002, China

[d] The Forth People Hospital of Changsha, Changsha 41000, China

Outline

1. Materials and methods

Materials. All reagents and solvents were used as received from commercial suppliers. All aqueous solutions were prepared with distilled water. MB49 and RS1 cell lines were obtained from American Type Culture Collection (ATCC)

Purification and characterization techniques. Flash column chromatography was conducted with 200–300 mesh silica. UV–vis spectra were recorded in a quartz cell (light path = 1 cm) on a CARY5000 spectrophotometer. ^{1}H NMR spectra were recorded on a QUANTUM-I-400 MHz spectrometer. TEM pictures were obtained on an FEI Talos microscope at an accelerating voltage of 200 kV. Fluorescence emission spectra were measured on a FLUOROMAX-4 fluorescence spectrophotometer. SEM pictures were obtained with a JSM-7500F scanning electron microscope.

MTT assay. The medium containing the cells at a density of 8×10^4 was seeded in the 96-well plates, in which 100 μL medium was placed per well, and the plates were cultured at 37 °C for 12 h at an atmosphere of 5% CO_2. Then the serial solutions containing the test molecules, and the assembly were added to the plates, which were further incubated for a different time. After that, the culture medium was removed, followed by the addition of 100 μL of MTT solution, which was incubated at 37 °C for another 4 h. Then the MTT formazan crystals were formed and dissolved by dimethyl sulfoxide (DMSO, 75 μL). Finally, the OD value at 490 nm was recorded by a microplate reader (BioTek ELx808). The cells cultured in the fresh medium were set as the control group. The cytotoxicity was presented as the relative percentage of the cell viability compared with the control group.

Colocalization experiment. The MB49 cells were seeded in plates at a density of 2×10^5 cells per well in 0.5 mL of complete culture medium for 12 h before treatment, which were further treated with **PDI-NH$_2$**. For MB49 cells, the mitochondria were further labeled by Mito-Tracker Green according to the provided instructions. Then, the cells were investigated by fluorescence microscopy (A1, Nikon, or STELLARIS 5, Leica).

***In vitro* ROS imaging.** The MB49 cells were seeded in plates at a density of 2×10^5 cells per well in 0.5 mL of complete culture medium for 12 h before treatment, which were further treated with **PDI-NH$_2$** for 12 h. After the removal of culture media, the DCFDA solution were added according to the provided instructions. Then, the cells were investigated by fluorescence microscopy (A1, Nikon).

***In vitro* LPO imaging.** The MB49 cells were seeded in plates at a density of 2×10^5 cells per well in 0.5 mL of complete culture medium for 12 h before treatment, which were further treated with **PDI-NH$_2$** for 12 h. After the removal of culture media, the solution containing BODIPY™ 581/591 C11 was added according to the provided instructions. Then, the cells were investigated by fluorescence microscopy (A1, Nikon).

Monitoring the mitochondrial membrane potential. The MB49 cells were seeded in plates at a density of 2×10^5 cells per well in 0.5 mL of complete culture medium for 12 h before treatment, which were further treated with **PDI-NH$_2$** for 12 h. After the removal of culture media, the solution containing JC-1 was added according to the provided instructions. Then, the cells were investigated by fluorescence microscopy (A1, Nikon).

Western blot analysis. Normally, proteins from cells were extracted with RIPA tissue lysis buffer and then the protein concentration was determined by a BCA protein assay. Following this, after adding western loading buffer, the obtained proteins were deformed by heating at 100 °C for 10 min. Subsequently, the samples were separated by 10 % SDS-polyacrylamide gel and transferred

onto 0.22 μm PVDF membranes (Beyotime Biotechnology Co., Ltd., Shanghai, China). After this, the obtained membranes were sealed with 5 % skim milk for 1 h at room temperature. Afterward, the membranes were incubated with the corresponding primary rabbit anti-mouse β-actin antibody (1:4000, Affinity, USA), Rabbit monoclonal antibody to GPX4 antibody (1:1000, Cell Signaling Technology, USA) at 4◦C overnight. The PVDF membranes were then incubated with goat anti-rabbit IgG (H + L) Horse Radish Peroxidase (HRP) (dilution 1:5000, Affinity Biosciences Inc., USA) for 1 h at room temperature. Finally, the signals were detected using a fluorescence and chemiluminescence gel imaging system (Peiqing Technology, Shanghai, China). All normalized protein expressions were processed and quantified by ImageJ and GraphPad Prism 7.0 software.

RNA-sequencing analysis. The total RNA was extracted from two groups of cells (pure culture medium as control group and **PDI-NH$_2$** as case group) by Trizol (Beyotime Technology, China). Then, the obtained RNA were quantified by spectrophotometer NanoPhotometer (IMPLEN, CA, USA) and qualified by Agilent 2100 bioanalyzer (Agilent Technologies, CA, USA). The RNA sequencing libraries were generated when total RNA concentration was above 50 ng/mL, OD=1.8~2.2, and RIN (mRNA integrity number) ≥ 7. The RNA purification, reverse transcription and sequencing were accomplished in Shanghai OE Biotech Co. Ltd. Fragments Per Kilobase Million (FPKM) was calculated to estimate gene expression levels. Differentially expressed genes (DEGs) were determined using limma package with P value < 0.05 and |logFC| > 0.56. The Gene Oncology (GO) and KEGG enrichment analysis were performed to explore the function of DEGs using GO-Term Finder and the Database for Annotation, Visualization and Integrated Discovery (DAVID) tools.

Bio-TEM. MB49 cells were co-incubated with **PDI-NH$_2$** for 24h, respectively. The incubated cells were trypsinized and washed with PBS buffer before being fixed in glutaraldehyde (2.5%) overnight. The cells isolated from the fixing solution were washed by PBS buffer for 15 min (3 times) and further fixed by the solution of citric acid (1%) for 2h. Subsequently, the cells were washed with PBS buffer (3 times) and dehydrated with the mixtures of ethanol and PBS in a ratio gradient ranging from 30%, 50%, 70%, 80%, 90%, to 95%) for 15 min in each case and neat ethanol and acetone for 20 min, respectively. The dehydrated cells were immersed in the EPON 812 resin washed with acetone. Sectioning the cells by a LEICA EM UC7 ultrathin slicer into 70-90 nm sections, which were further stained by the solution of lead citrate and the saturated solution of uranyl acetate in 50% ethanol for 10 min, respectively. Eventually, the bio-TEM images of the cells were recorded by FEI Talos microscope.

Statistical analysis. The results were expressed in the form of mean ± standard deviation, in which at least three independent experiments were performed for the results. Tukey's test (Origin 8.0) was used for One-way analysis of variance. *P < 0.05 was considered to be statistically significant.

***In vivo* anti-tumor experiment**. To investigate the anti-tumor behavior *in vivo*, the MB49 tumor model was established. Generally, Balb/C mice were injected subcutaneously with 5×10^6 MB49 cells. Two weeks later, the mice bearing approximately 90 mm^3 tumors were randomly divided into two groups (n = 5). **PDI-NH$_2$** (4 mg/mL) was *in situ* administered 50 μL every days for 10 days and control mice were injected with the same volume of saline. During the treatment, no mice died in all groups. We measured the tumor volume and body weight of mice every two days, and the calculation of tumor volumes was according to the formula: Tumor volume (mm^3) = 0.5 × (Tumor width)^2 × Tumor length. Finally, the mice were euthanized and the tumors were resected, taken photographs and weighed. The harvested tumor tissues and major organs (lung, heart spleen, liver,

and kidney) were fixed using 4% para-formaldehyde for hematoxylin and eosin (H&E), Tunel, Ki67 staining. The animal experiments were approved by the Science and Technology Department of Jiangsu Province and conducted with the approval of the Medical Ethics Committee of Yangzhou University Medical Academy (YXYLL-2022-44).

***In vivo* safety evaluation**. To investigate the safety of **PDI-NH$_2$** *in vivo*, the solution of **PDI-NH$_2$** in PBS (100 μL) was injected into the Balb/C mice through the tail vein. The blood was collected after 24 h respectively for the biochemical analysis, and major organs (lung, heart spleen, liver, and kidney) after 10 day for hematoxylin and eosin (H&E) staining. The animal experiments were approved by the Science and Technology Department of Jiangsu Province and conducted with the approval of the Medical Ethics Committee of Yangzhou University Medical Academy (YXYLL-2022-44).

2. Synthesis of PDI-NH$_2$

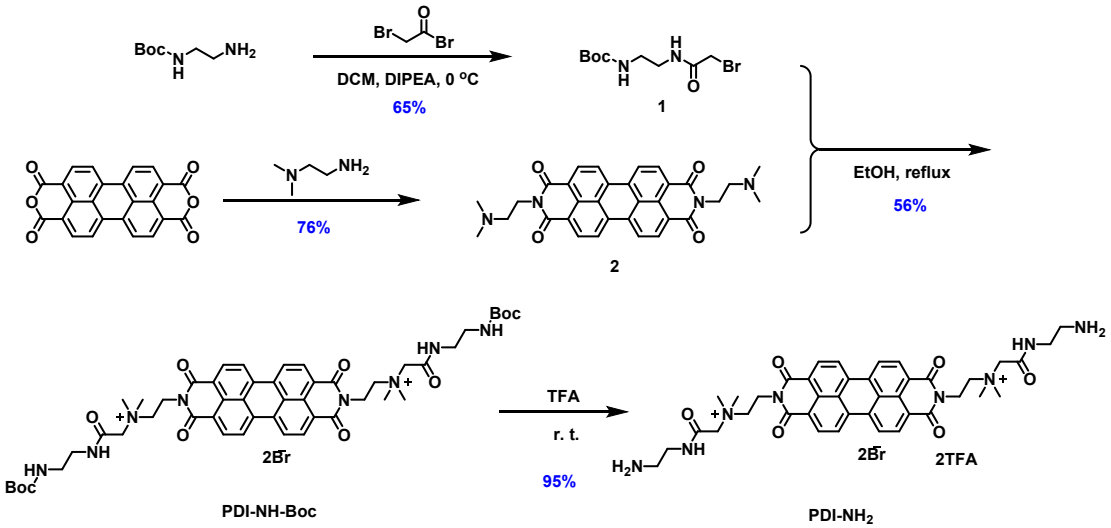

Scheme S1. Synthesis route of **PDI-NH$_2$**.

1: The N-Boc-Ethylenediamine (0.48 g, 3 mmol) was dispersed in anhydrous dichloromethane (20 mL) with anhydrous DIPEA (1 mL), then this solution was cooled in ice bath for 20 min, followed by the drop-wise addition of the dichloromethane solution (10 mL) containing bromoacetyl bromide (1.20 g, 6 mmol). After the addition of bromoacetyl bromide solution, the ice bath was removed, and the reaction was kept at room temperature for 12 h. The final solution was washed with water (2 × 30 mL), and followed by brine (40 mL) and dried with Na_2SO_4. The organic layer was evaporated in vacuo resulting in the crude product, which was further subjected to silica gel chromatography (dichloromethane) to give the target compound **1** as the white solid (0.55 g, 1.95 mmol, 65% yield). M.p. 116−118 °C. ^{1}H NMR (400 MHz, $CDCl_3$, 298 K) δ (ppm): 7.23 (br, 1H), 5.07 (br, 1H), 3.87 (s, 2H), 3.41, (s, 2H), 3.32 (s, 2H), 1.46 (s, 9H). ^{13}C NMR (101 MHz, $CDCl_3$, 298 K) δ (ppm): 166.5, 156.9, 80.0, 41.5, 39.9, 29.0, 28.5. HR-ESI-MS: *m/z* Calcd. For $C_9H_{17}BrN_2NaO_3^+$ $[M+Na]^+$ 303.0315, found 303.0318.

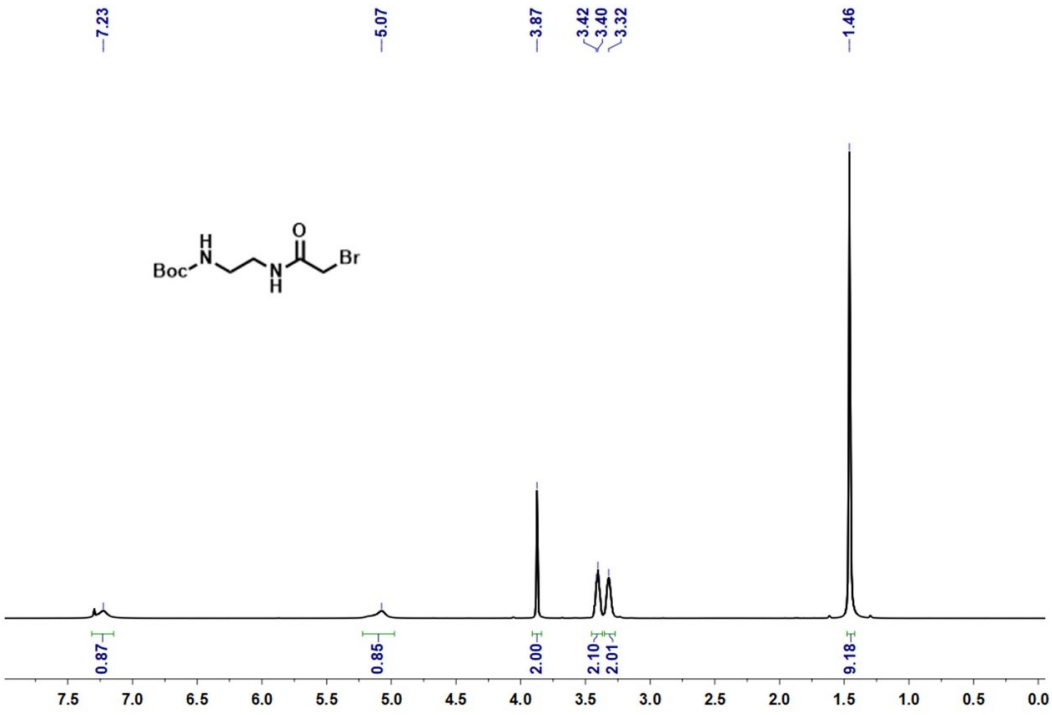

Figure S1. ^{1}H NMR (400 MHz, $CDCl_3$, 298 K) spectrum of compound **1**.

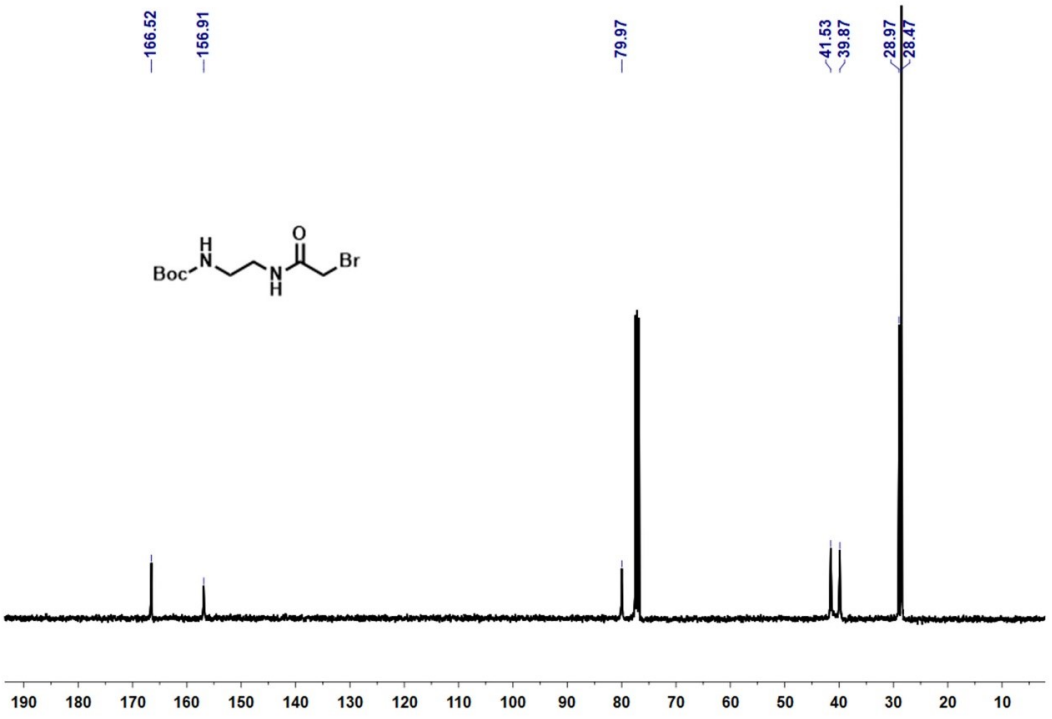

Figure S2. ^{13}C NMR (101 MHz, $CDCl_3$, 298 K) spectrum of compound **1**.

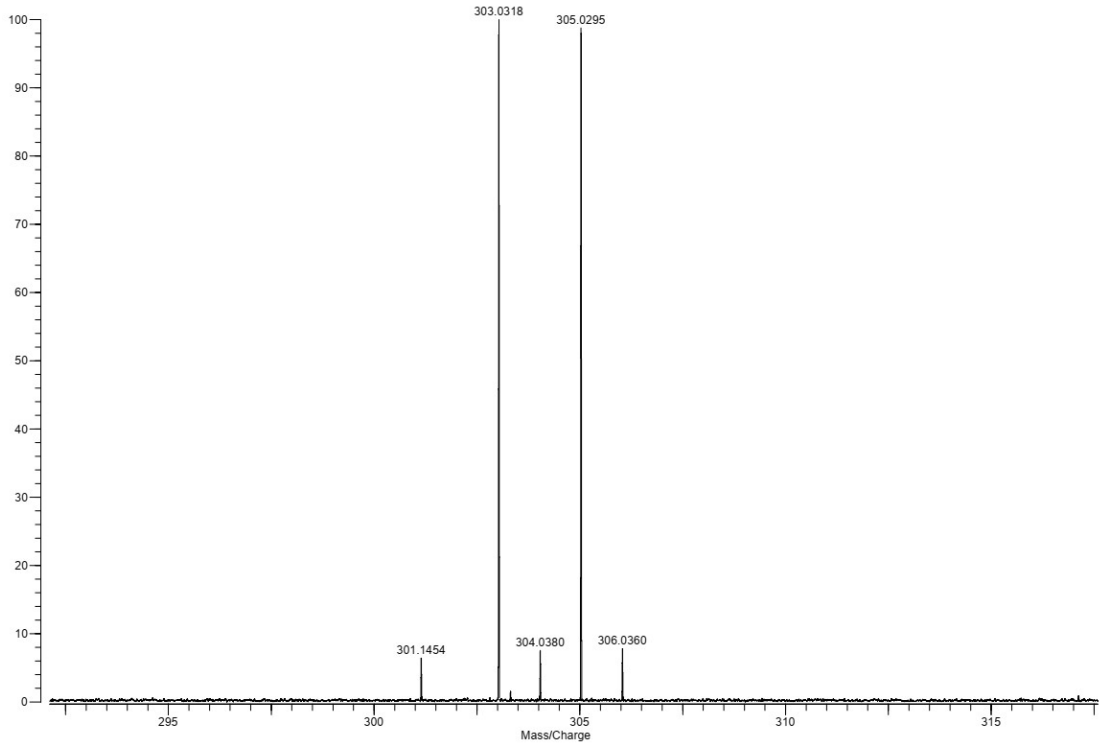

Figure S3. HR-MS spectrum of compound **1**.

2[S1]: Perylene-3,4,9,10-tetracarboxylic dianhydride (2.5 g, 6.4 mmol) and N,N-dimethylethylenediamine (4 mL, 20 mmol) were added into DMF (25 mL), and the solution was stirred at 130 °C for 5 h. After the reaction, the reaction bath was cooled to room temperature, and cold THF (150 mL) was poured into the reaction bath. The precipitate was filtered, and the residue was washed with THF several times to obtain the product 1 as a dark brown solid (3.59 g, 4.86 mmol, 92% yield). ^{1}H NMR (400 MHz, D_2O, 298 K) δ (ppm): 7.84 (br, 8H), 4.42 (s, 4H), 3.53 (s, 4H), 3.05 (s, 12H).

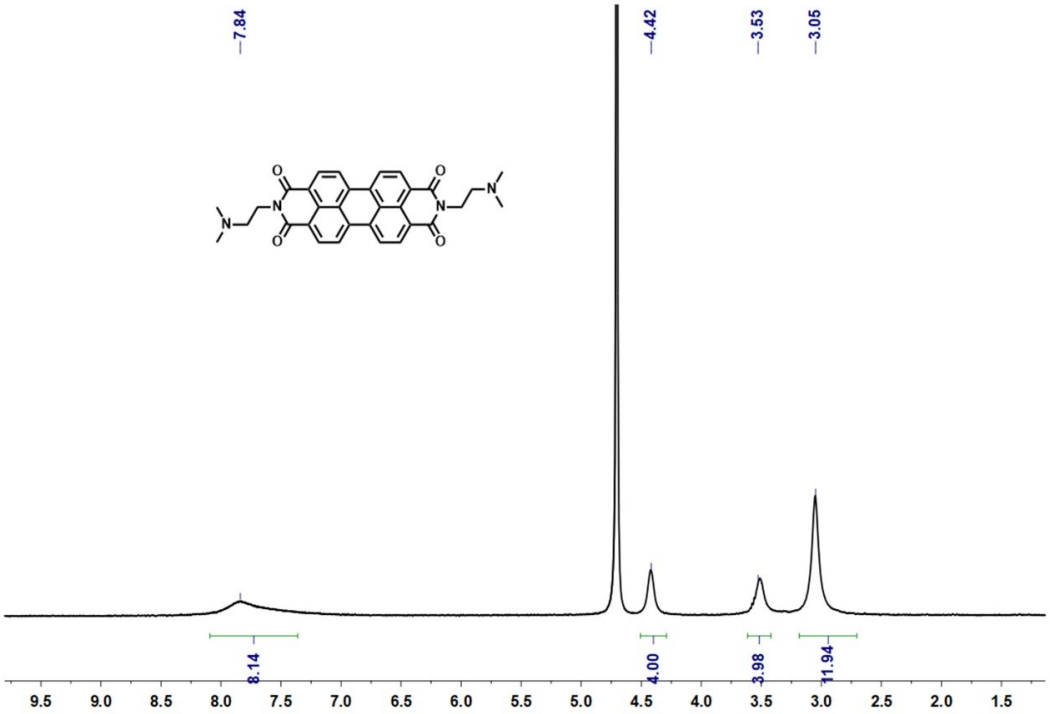

Figure S4. ^{1}H NMR (400 MHz, D_2O, 298 K) spectrum of compound **2** (1% TFA).

PDI-NH-Boc: Compound **1** (1.12 g, 4 mmol) was added to the ethanol solution (30 mL) containing compound **2** (1.06 g, 2 mmol), then the mixture was refluxed for 48 h in the atmosphere of Ar. After that, the solvent was removed to afford the dark red solid. And the residue was purified by Al_2O_3 chromatography to obtain the target compound as a dark red solid (1.23 g, 1.13 mmol, 56% yield). M.p. >300 ^{o}C. ^{1}H NMR (400 MHz, DMSO-d_6, 298 K) δ (ppm): 8.86 (s, 2H), 8.80 (d, J = 8.1 Hz, 4H), 8.51 (d, J = 8.1 Hz, 4H), 6.90 (t, J = 5.6 Hz, 2H), 4.57 (s, 4H), 4.31 (s, 4H), 3.92 (t, J = 6.7 Hz, 4H), 3.44 (s, 12H), 3.17–3.11 (m, 4H), 3.03 (d, J = 6.1 Hz, 4H), 1.36 (s, 18H).^{13}C NMR (101 MHz, DMSO-d_6, 298 K) δ (ppm): 163.8, 162.6, 156.1, 133.4, 130.6, 127.8, 124.4, 124.2, 121.8, 99.9, 78.3, 63.0, 61.3, 52.2, 39.5, 34.2, 28.8. HR-ESI-MS: *m/z* Calcd. For $C_{50}H_{62}N_8O_{10}^{2+}$ $[M\text{-}2Br]^{2+}$ 467.2289, found 467.2293.

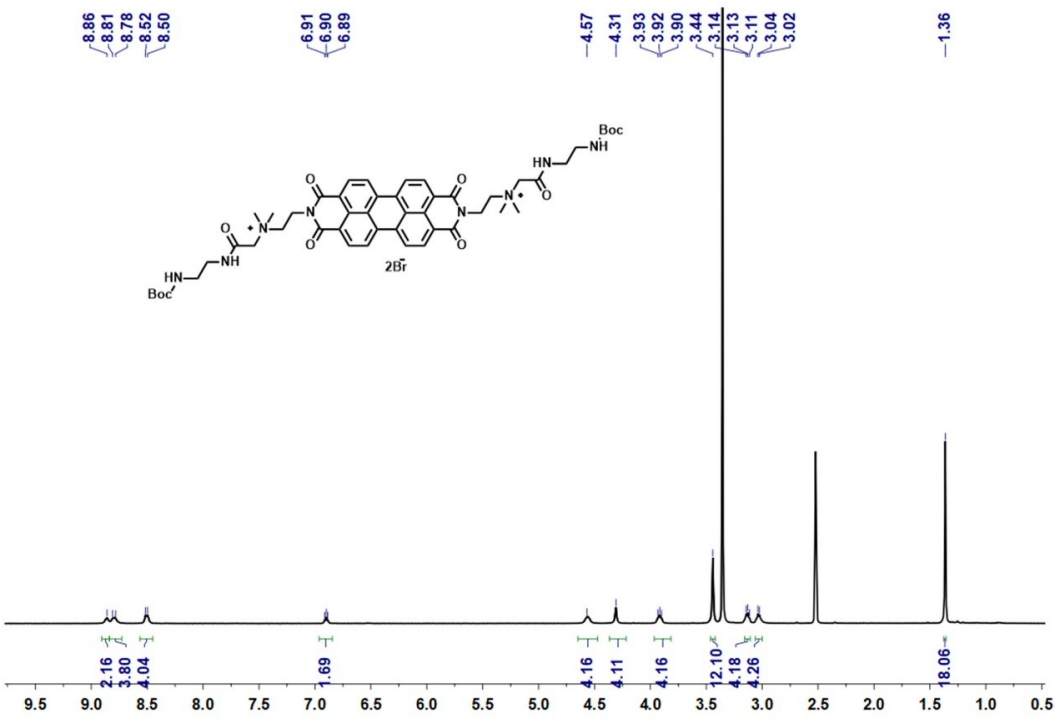

Figure S5. ^{1}H NMR (400 MHz, DMSO-d_6, 298 K) spectrum of **PDI-NH-Boc**.

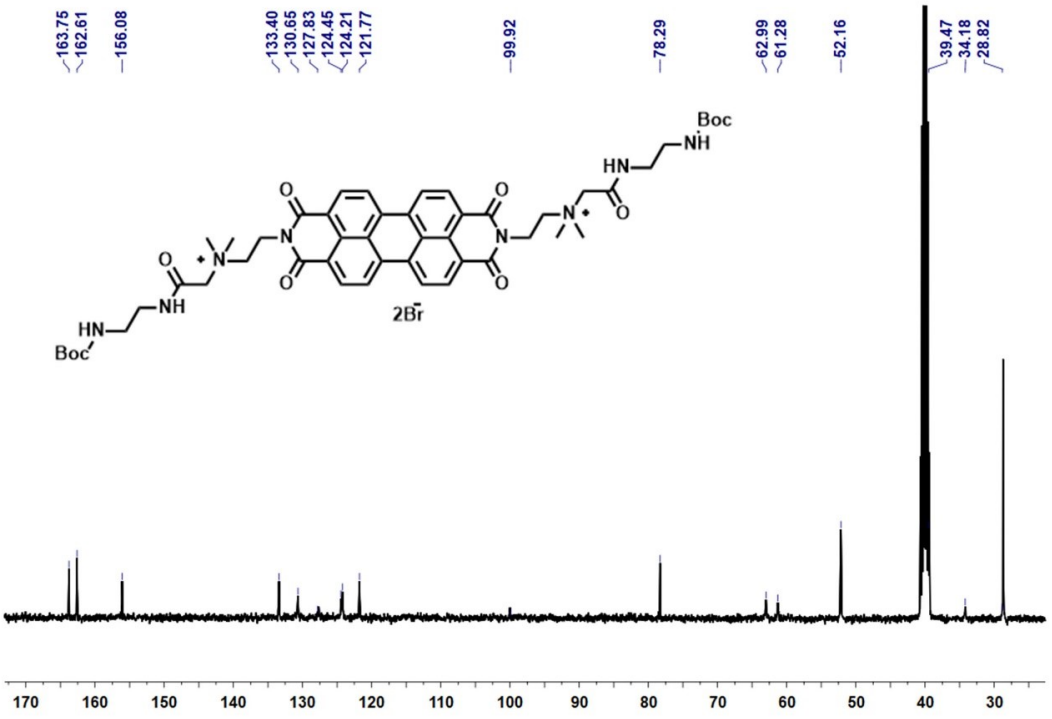

Figure S6. ^{13}C NMR (101 MHz, DMSO-d_6, 298 K) spectrum of **PDI-NH-Boc**.

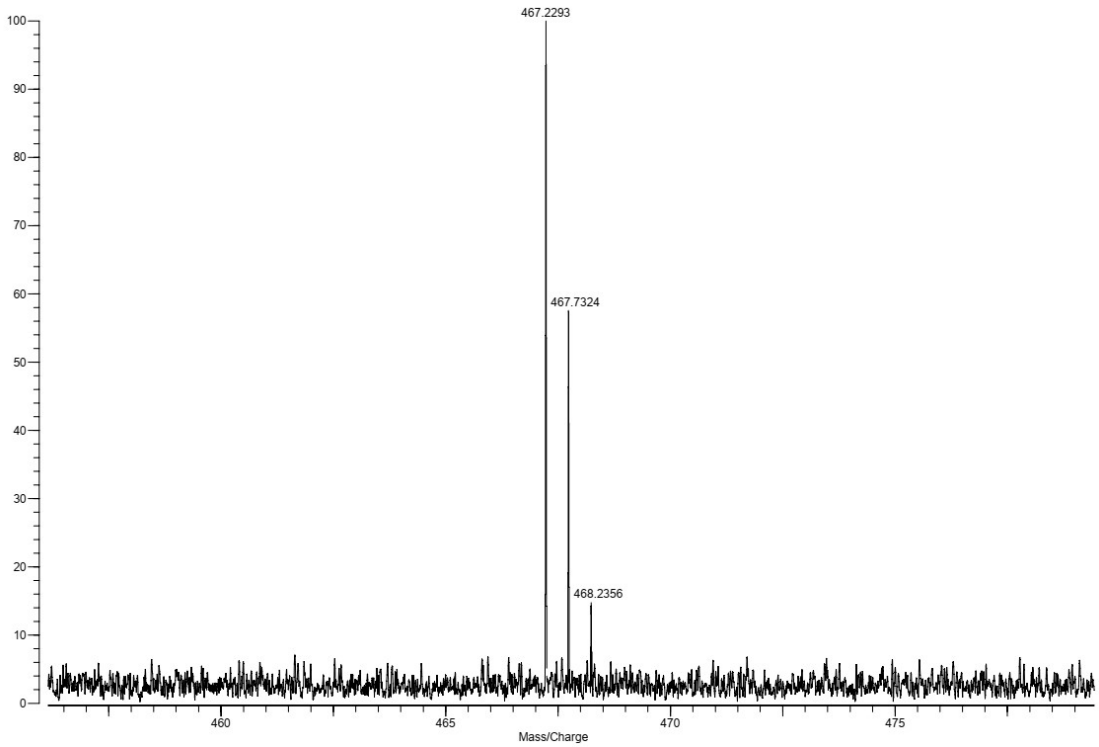

Figure S7. HRMS spectrum of **PDI-NH-Boc**.

PDI-NH_2: **PDI-NH-Boc** (1.10 g, 1mmol) was added into trifluoroacetic acid solution (10 mL), and the mixture was stirred at room temperature for 12 h. Then the solvent was removed under reduced pressure and washed with toluene (20 mL × 3). The target compound was obtained as a dark red solid (1.06 g, 0.95 mmol, 95% yield). M.p. >300 °C. ^{1}H NMR (400 MHz, DMSO-d_6, 298 K) δ (ppm): 9.05 (d, J = 8.2 Hz, 4H), 8.88 (t, J = 5.6 Hz, 2H), 8.67 (d, J = 7.9 Hz, 4H), 7.88 (s, 6H), 4.55 (s, 4H), 4.27 (s, 4H), 3.93–3.83 (m, 4H), 3.45–3.33 (m, 16H), 2.95 (dd, J = 11.9, 5.9 Hz, 4H).^{13}C NMR (101 MHz, DMSO-d_6, 298 K) δ (ppm): 164.38, 162.98, 159.16, 134.04, 131.11, 128.37, 125.22, 124.49, 122.42, 122.42, 118.63, 115.71, 62.89, 61.02, 52.19, 38.55, 37.02, 34.06. HR-ESI-MS: *m/z* Calcd. For $C_{40}H_{46}N_8O_6^{2+}$ $[M\text{-}2Br\text{-}2TFA]^{2+}$ 367.1765, found 367.1786.

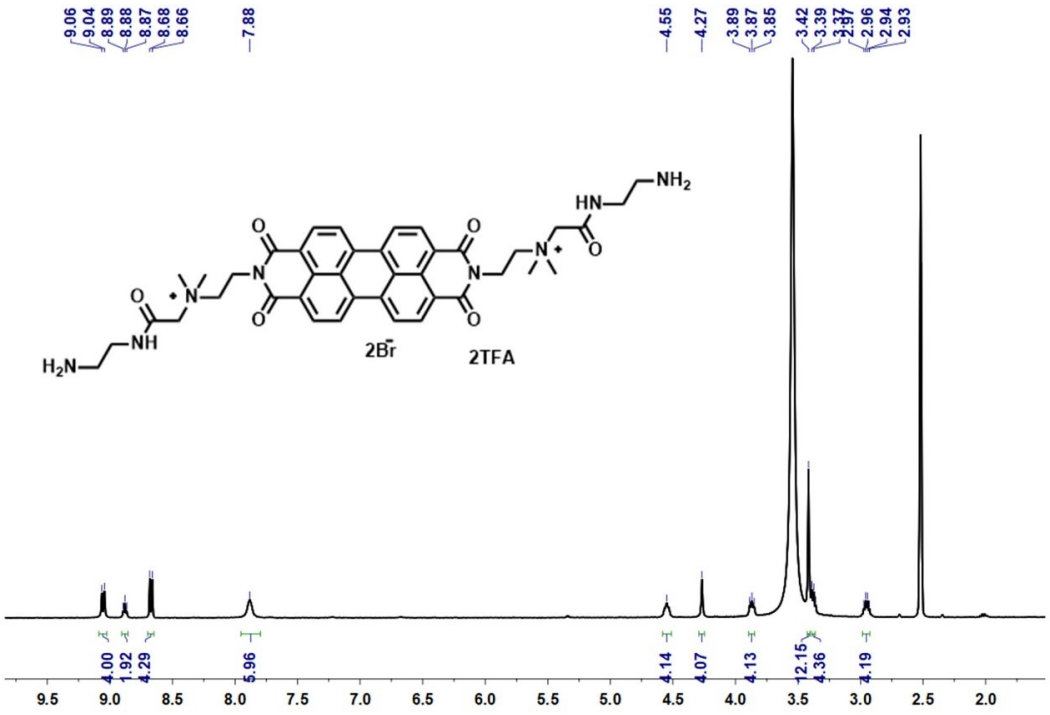

Figure S8. ^{1}H NMR (400 MHz, DMSO-d_6, 298 K) spectrum of **PDI-NH$_2$**.

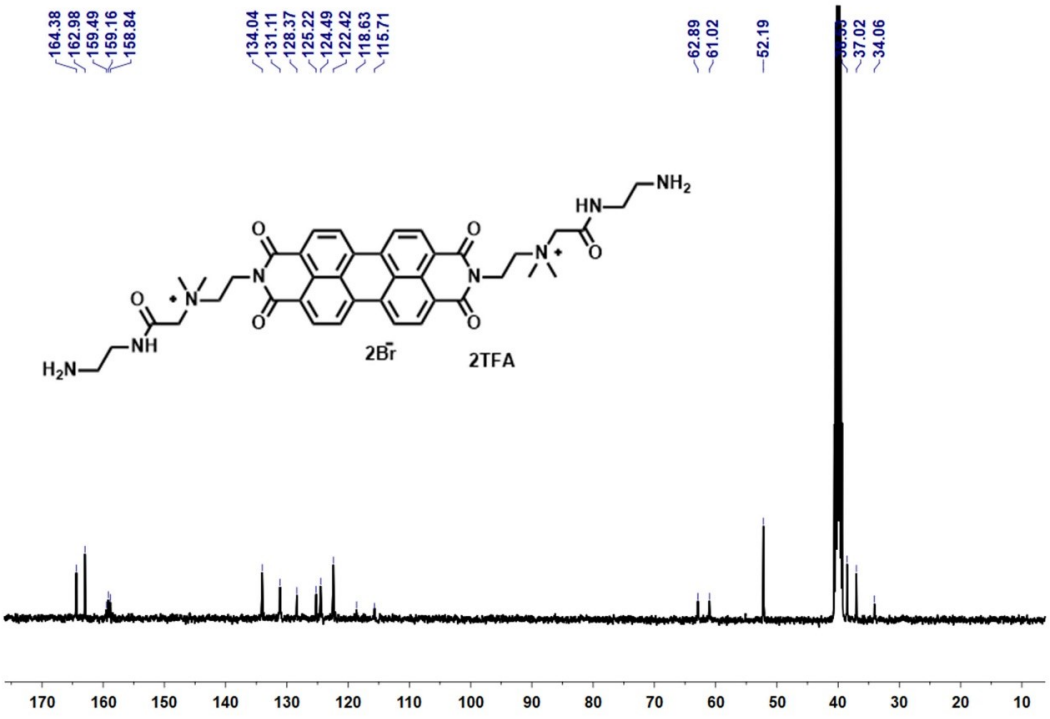

Figure S9. ^{13}C NMR (101 MHz, DMSO-d_6, 298 K) spectrum of **PDI-NH$_2$**.

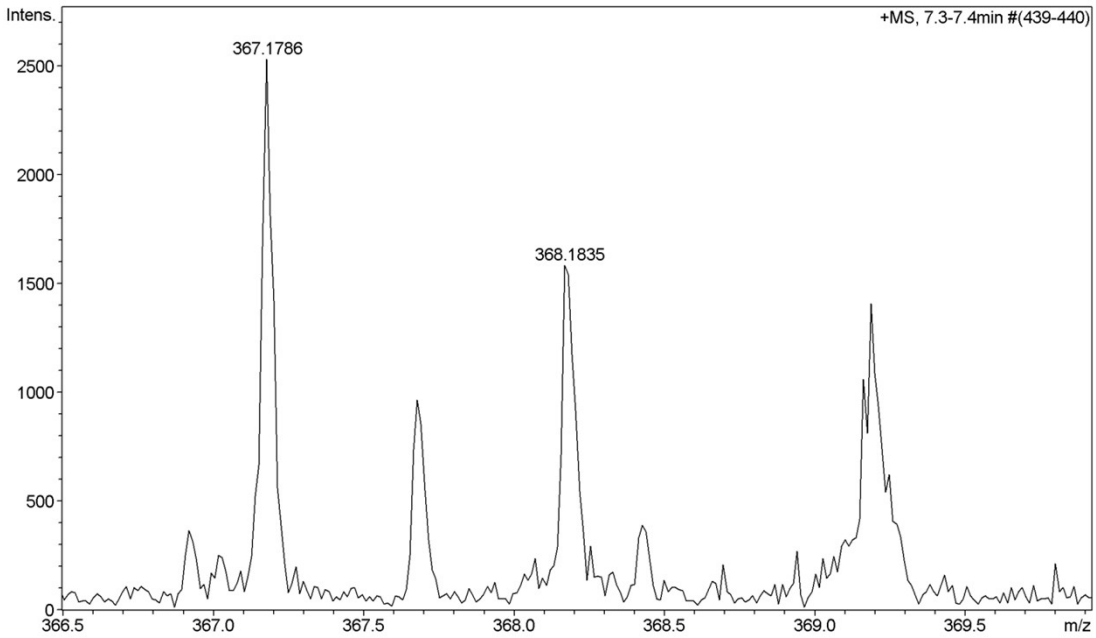

Figure S10. HR-MS spectrum of **PDI-NH$_2$**.

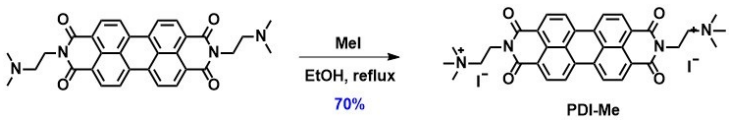

Scheme S2. Synthesis route of **PDI-Me**.

PDI-Me[S2]: Iodomethane (1.41 g, 10 mmol) was added to the ethanol solution (30 mL) containing compound **2** (1.06 g, 2 mmol), then the mixture was refluxed for 48 h in the atmosphere of Ar. After that, the solvent was removed to afford the dark red solid. And the residue was purified by Al_2O_3 chromatography to obtain the target compound as a dark red solid (1.13 g, 1.39 mmol, 70% yield). ^{1}H NMR (400 MHz, DMSO-d_6, 298 K) δ (ppm): 8.69 (d, J = 8.2 Hz, 4H), 8.46 (d, J = 7.9 Hz, 4H), 4.56–4.47 (m, 4H), 3.46–3.37 (m, 4H), 3.26 (s, 18H).

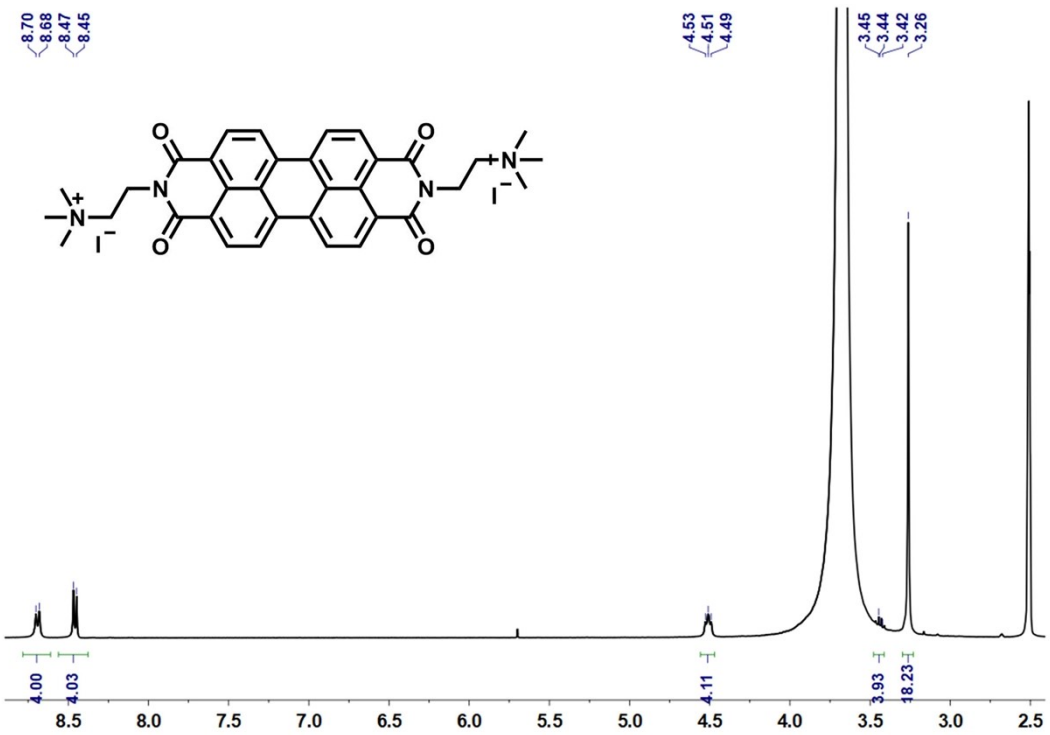

Figure S11. ^{1}H NMR (400 MHz, DMSO-d_6, 298 K) spectrum of **PDI-Me**.

3. Optical transmittance curves of PDI-NH_2.

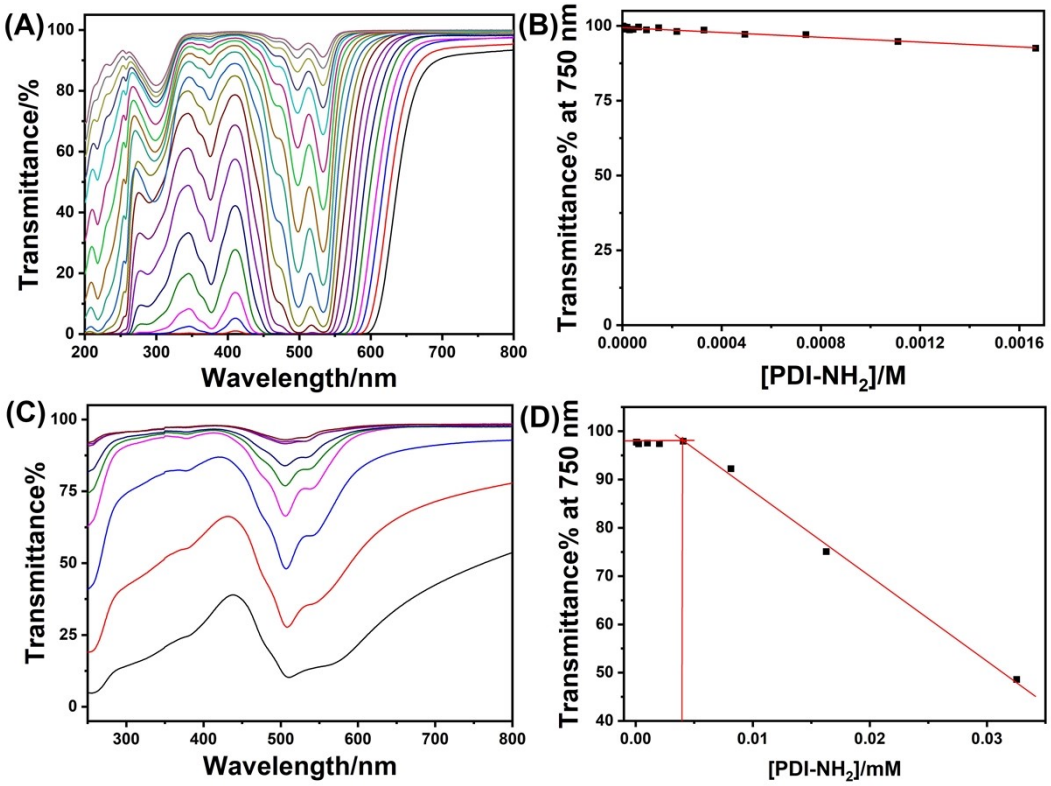

Figure S12. (A) Concentration-dependent optical transmittance curves of **PDI-NH_2**, (B) CAC curve of **PDI-NH_2**. (C) Concentration-dependent optical transmittance curves of **PDI-NH_2** in presence of ATP ([**PDI-NH_2**]:[**ATP**] = 1:1.6), (D) CAC curve of **PDI-NH_2** in presence of **ATP**.

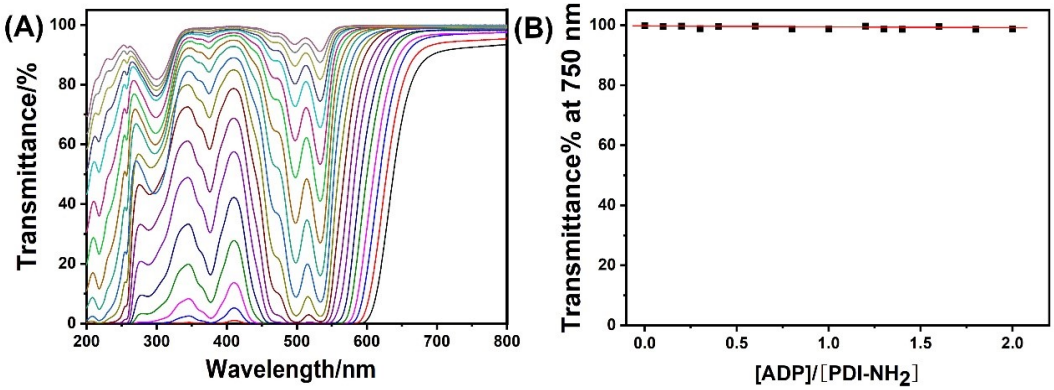

Figure S13. (A) Optical transmittance curves of **PDI-NH_2** in the presence of variant **ADP**, (B) Optical transmittance of **PDI-NH_2** at 750 nm in the presence of variant **ADP**.

4. UV-Vis and fluorescence spectra of PDI-NH_2 and PDI-Me in presence of multi-negatively charged molecules

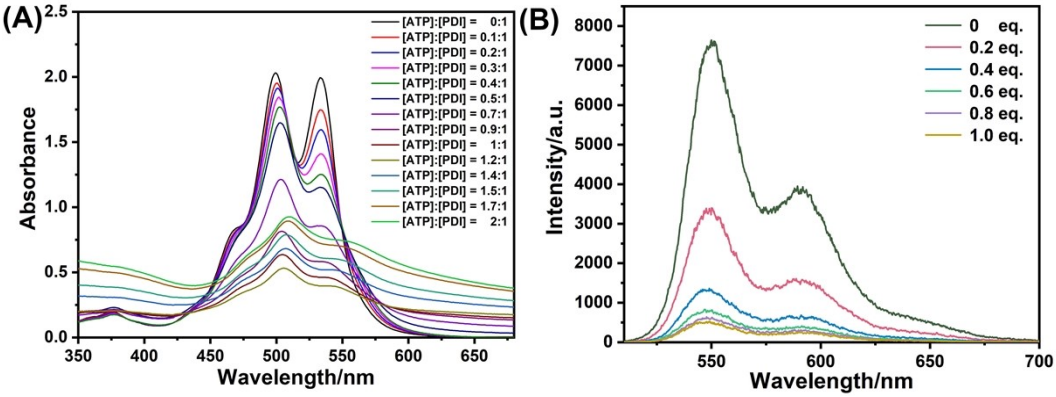

Figure S14. (A) UV-vis spectra of **PDI-NH_2** in presence of variant concentrations of **ATP** ([**PDI-NH_2**] = 0.02 mM), (B) fluorescence spectra of **PDI-NH_2** in presence of variant concentrations of **ATP** ([**PDI-NH_2**] = 0.02 mM).

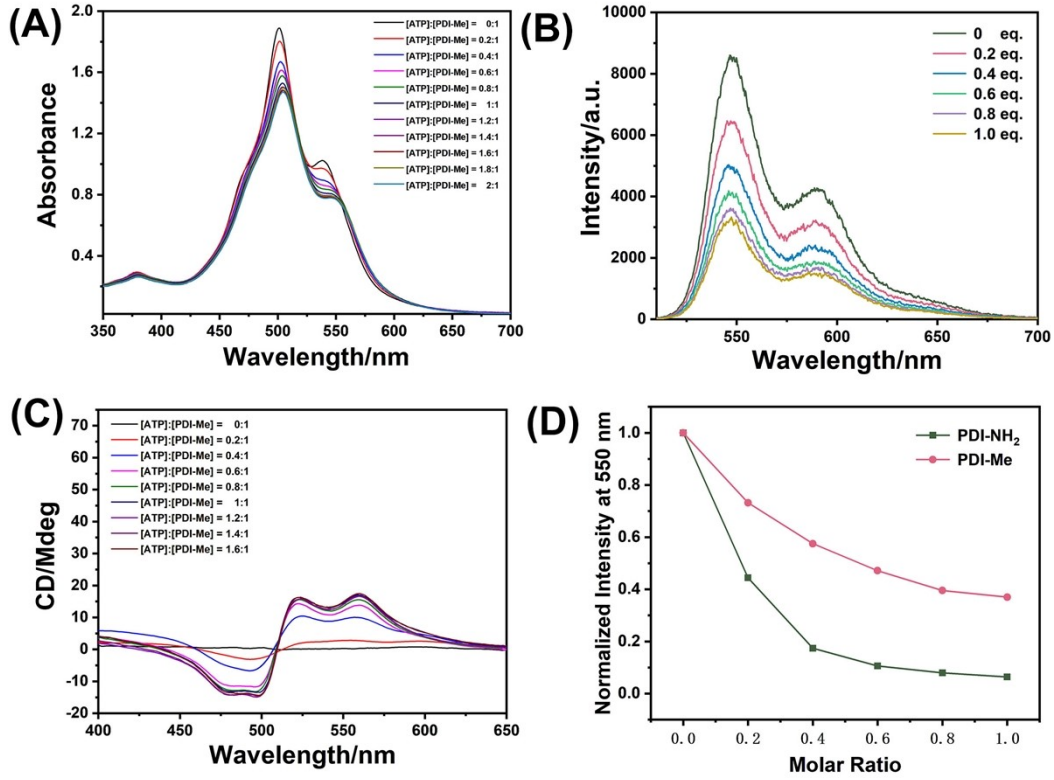

Figure S15. (A) UV-vis spectra of **PDI-Me** in presence of variant concentrations of **ATP** ([**PDI-Me**] = 0.02 mM), (B) fluorescence spectra of **PDI-Me** in presence of variant concentrations of **ATP** ([**PDI-Me**] = 0.02 mM), (C) CD spectra of **PDI-Me** in presence of **ATP** (**PDI-Me**] = 0.02 mM), (D) normalized fluorescence intensity at 550 nm in the presence of variant concentrations of **ATP** ((**PDI-Me**] = 0.02 mM, [**PDI-NH_2**] = 0.02 mM).

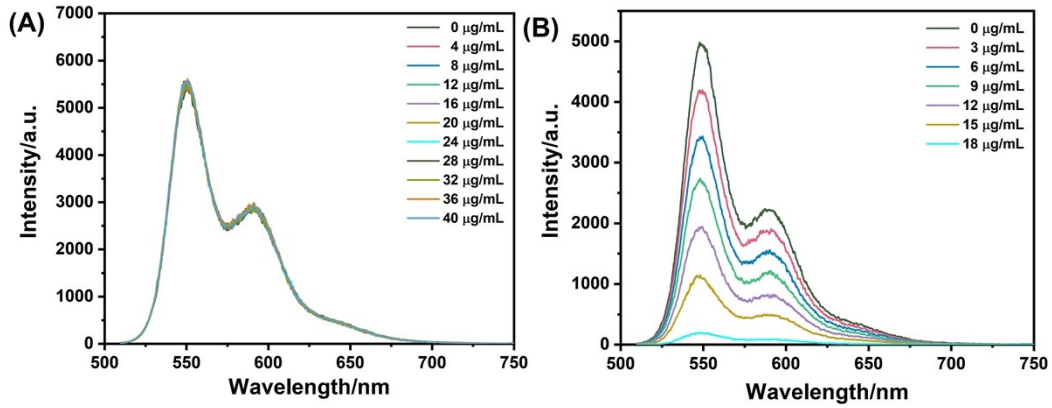

Figure S16. (A) Fluorescence spectra of **PDI-NH$_2$** in presence of variant concentration of BSA ([**PDI-NH$_2$**] = 0.02 mM), (B) fluorescence spectra of **PDI-NH$_2$** in presence of variant concentration of DNA ([**PDI-NH$_2$**] = 0.005 mM).

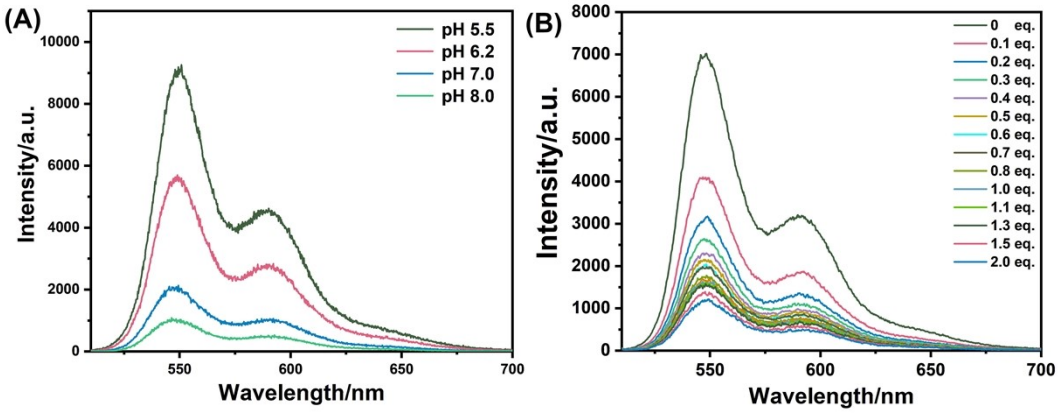

Figure S17. (A) Fluorescence spectra of **PDI-NH$_2$** in presence of variant concentration of ATP ([**PDI-NH$_2$**] = 0.02 mM, pH = 8)

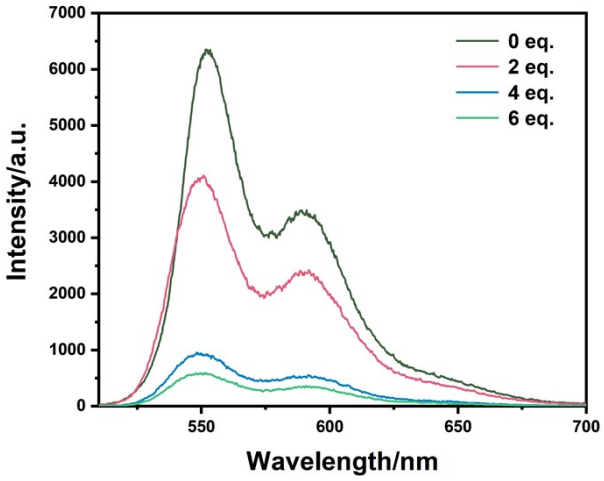

Figure S18. Fluorescence spectra of **PDI-NH$_2$** in presence of ADP ([**PDI-NH$_2$**] = 0.02 mM).

5. Self-assembly properties of PDI-Me and PDI-NH_2

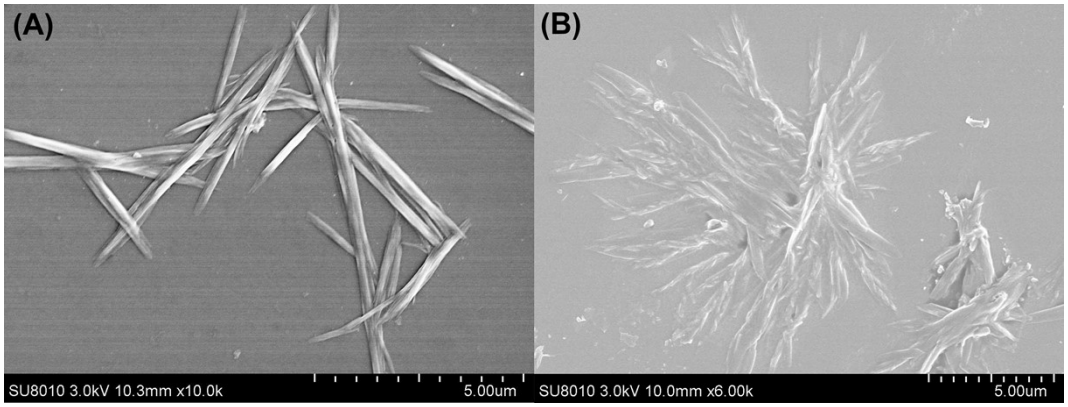

Figure S19. SEM images of (A) **PDI-Me**, and (B) **PDI-Me** and **ATP** (([**PDI-Me**]:[**ATP**] = 1:1.6)).

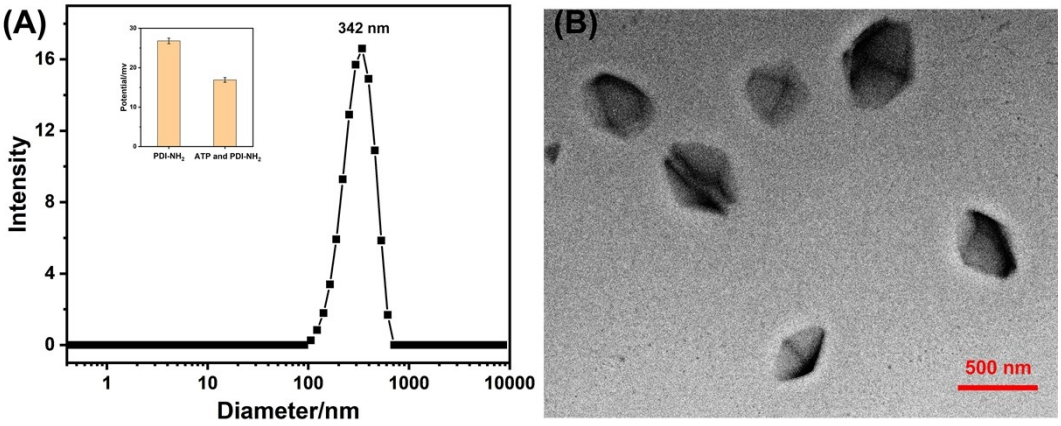

Figure S20. (A) DLS result of **PDI-NH_2** in the presence of **ATP** (insert: the zeta potential results of **PDI-NH_2** and **PDI-NH_2** in the presence of **ATP**), (B) TEM images of **PDI-NH_2** in the presence of **ATP**.

6. CD spectra of PDI-NH_2 in presence of ATP and ADP

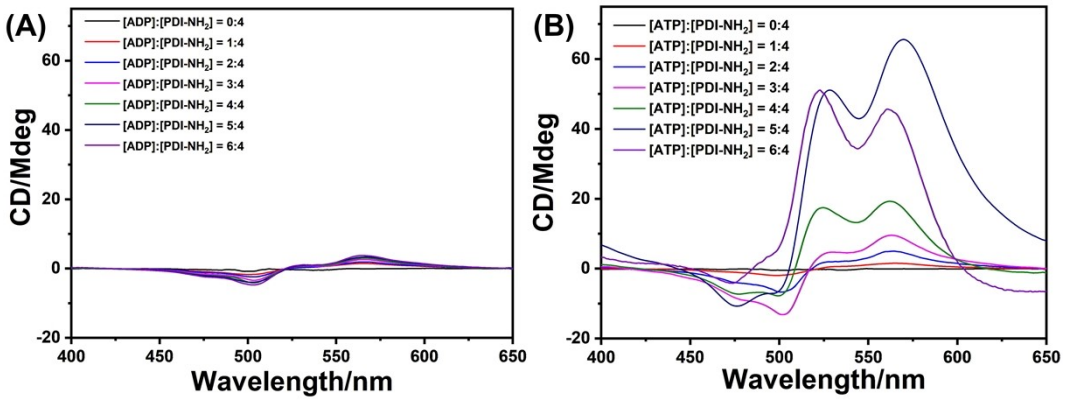

Figure S21. (A) CD spectra of **PDI-NH_2** in presence of **ADP** ([**PDI-NH_2**] = 0.02 mM), (B) CD spectra of **PDI-NH_2** in presence of **ATP** ([**PDI-NH_2**] = 0.02 mM).

7. Cell viability of MB49 cells in presence of PDI-Me

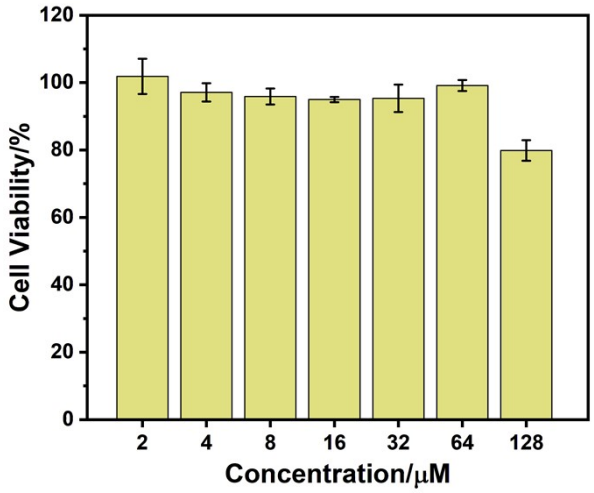

Figure S22. The concentration-dependent MTT assay of **PDI-Me** on MB49 cancer cells.

8. Colocation experiments of PDI-NH_2 in MB49 cancer cells

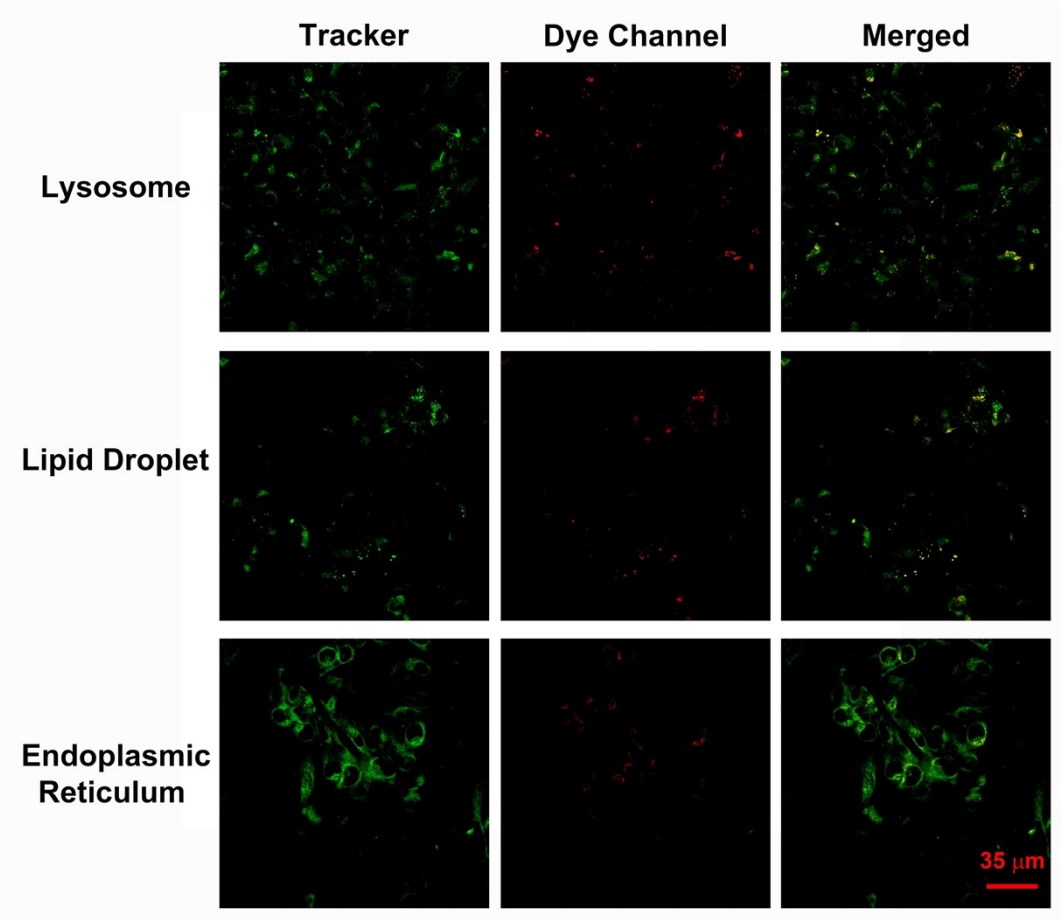

Figure S23. Confocal laser scanning images of **PDI-NH_2** in MB49 cancer cells.

9. Cellular uptake efficiency by flow cytometry

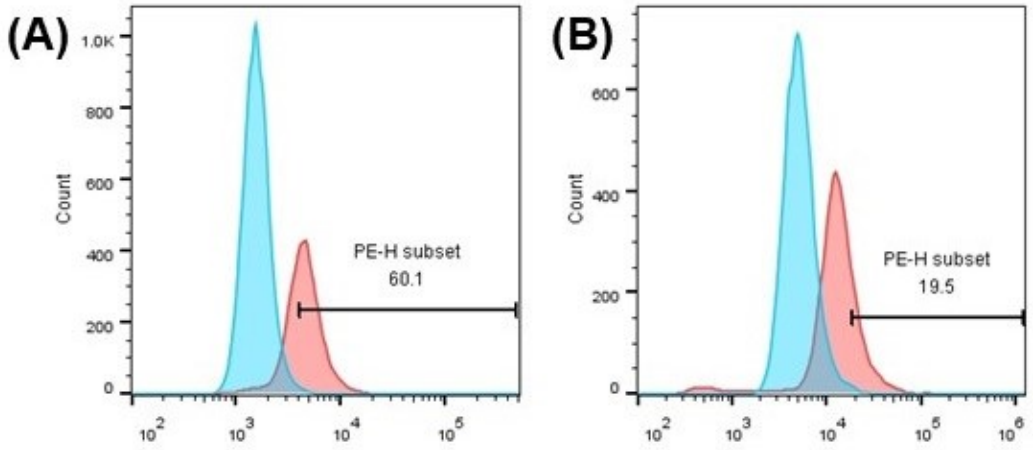

Figure S24. Fluorescence intensities of (A) MB49 cells and (B) RS1 cells were analyzed by flow cytometry after being incubated with **PDI-NH_2** for 12 h ([**PDI-NH_2**] = 5 μM, the fluorescence was collected in the channel of PE).

10. RNA-sequencing analysis of MB49

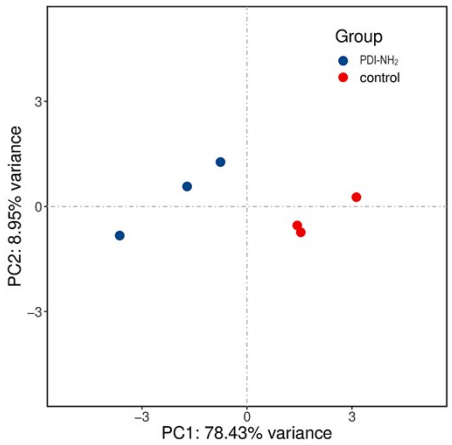

Figure S25. PCA evaluation based on the DEGs between control group and **PDI-NH$_2$**-treated group.

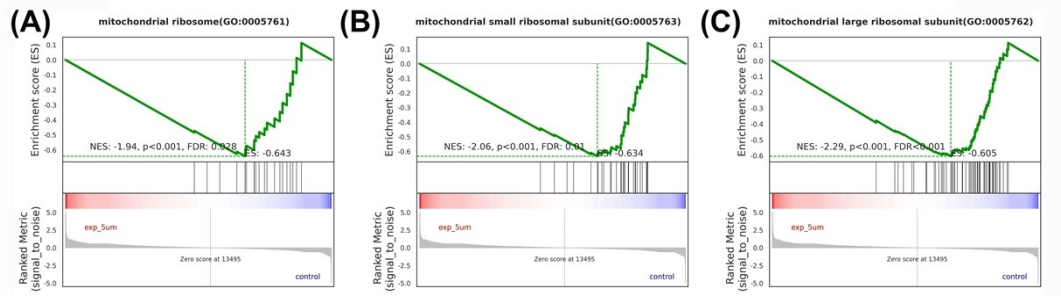

Figure S26. Gene set enrichment analysis (GSEA) enrichment plots of DEGs centralized in (A) mitochondrial ribosome, (B) mitochondrial small ribosome subunit, and (C) mitochondrial large ribosome subunit after **PDI-NH$_2$** treatment. ([**PDI-NH$_2$**] = 5 μM) .

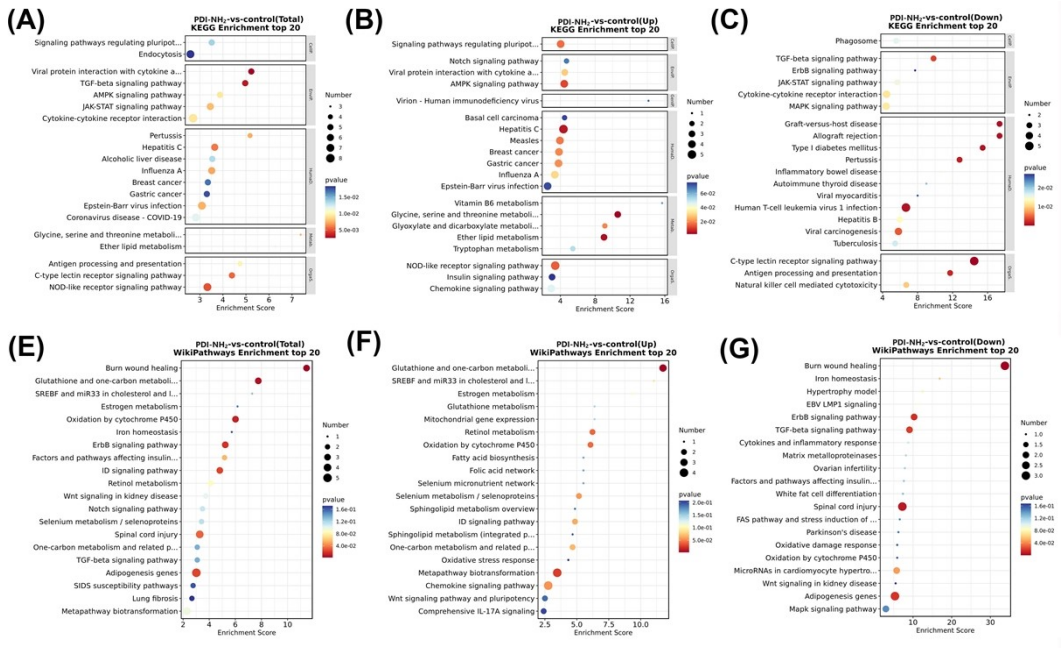

Figure S27. (A), (B), and (C) KEGG pathway enrichment analysis of DEGs based on RNA-seq after **PDI-NH$_2$** treatment. (D), (E), and (F) Wikipathway enrichment analysis of DEGs based on RNA-seq after **PDI-NH$_2$** treatment. ([**PDI-NH$_2$**] = 5 μM).

11. *In vitro* ROS imaging of MB49 cells in presence of PDI-NH_2

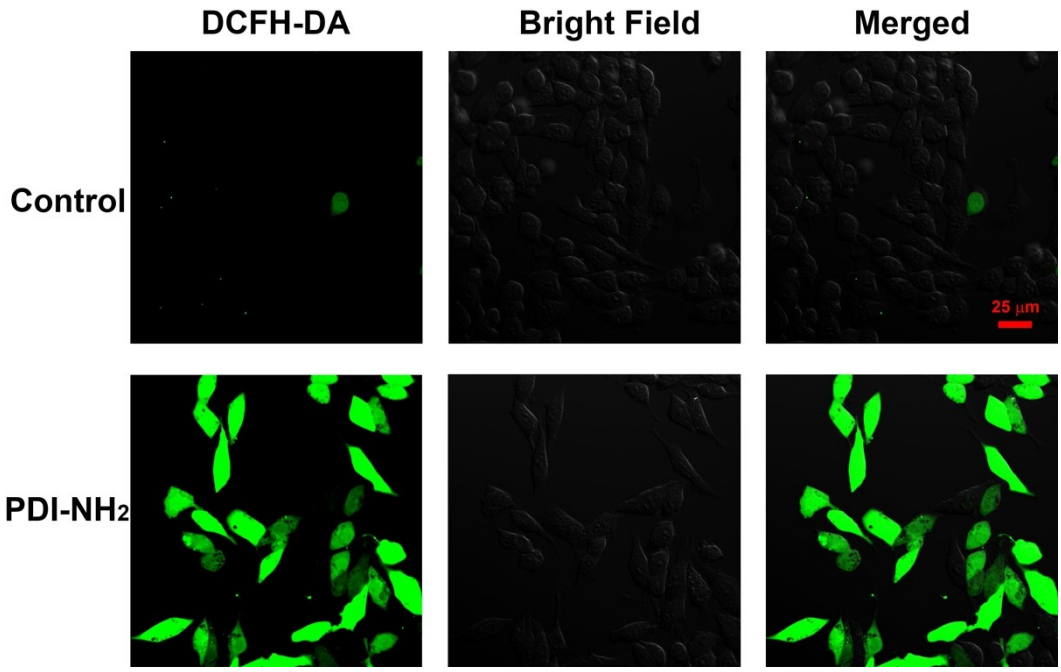

Figure S28. Fluorescence images of MB49 cancer cells stained by DCFHDA probe ([**PDI-NH_2**] = 10 μM).

12. *In vivo* biocompatibility analysis

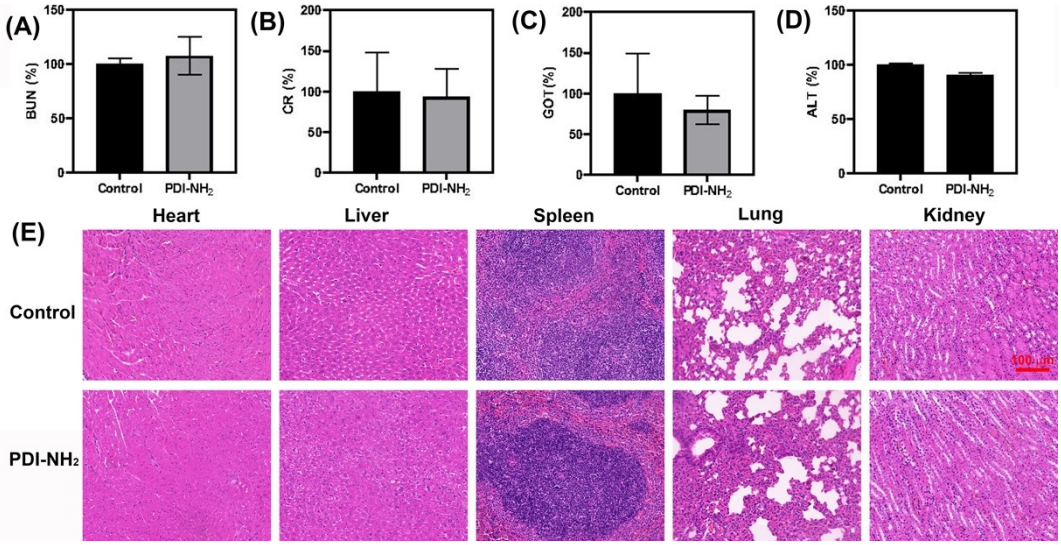

Figure S29. Serum biochemistry data of (A) BUN, (B) CR, (C) GPT, (D) GOT, and (E) ALT reflecting reflecting liver function and kidney function (n = 3), date were collected at 24 h after the tail vein injection, (C) H&E staining images of Liver, Heart, Spleen, Kidney, and Lung on Day 10.

13. The raw data of Western blot (WB)

The following pictures were the original photos (Figure S30 and S31) obtained from chemiluminescence gel imaging system (Peiqing Technology, Shanghai, China). The stripes from left to right represented the control group, 10 μM, 12 μM, 14 μM, 16 μM, 18 μM, and another repeated set. Due to the existence of bubble in the stripe of 18 μM (Figure 1), we could not accurately calculate the relative protein expression, so we clipped these photos shown in the text of Manuscript.

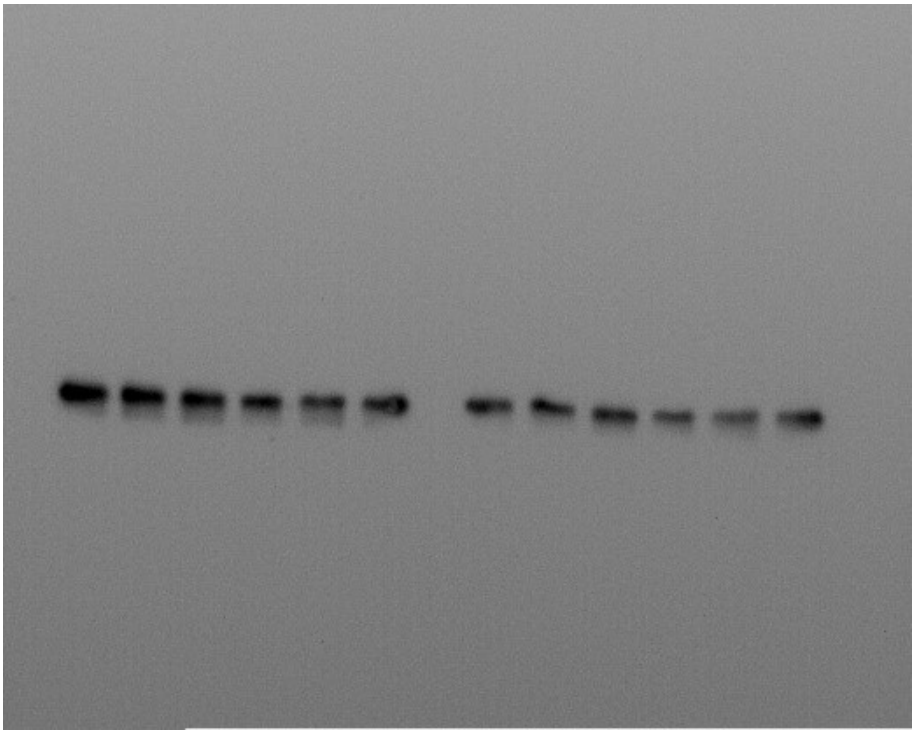

Figure S30. The gel image of GPX4 (Left)The stripes from left to right represented the control group, 10 μM, 12 μM, 14 μM, 16 μM, 18 μM, and (Right) another repeated set.

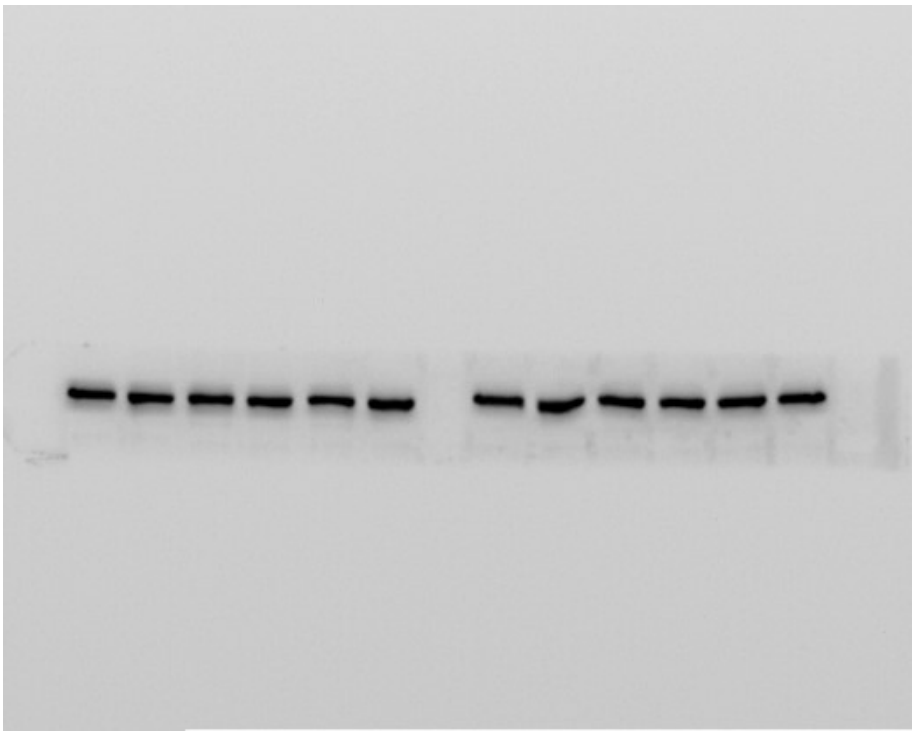

Figure S31. the gel image of β-actin The stripes from left to right represented the control group, 10 μM, 12 μM, 14 μM, 16 μM, 18 μM, and (Right) another repeated set.

14. Reference

[S1] F. Biedermann, E. Elmalem, I. Ghosh, W. M. Nau, and O. A. Scherman, Strongly Fluorescent, Switchable Perylene Bis(diimide) Host–Guest Complexes with Cucurbit[8]uril in Water, *Angew. Chem. Int. Ed.* **2012**, *51*, 7739.

[S2] Q. Chen, B. J. Worfolk, T. C. Hauger, U. Al-Atar, K. D. Harris, and J. M. Buriak, Finely Tailored Performance of Inverted Organic Photovoltaics through Layer-by-Layer Interfacial Engineering, *ACS Appl. Mater. Interfaces* **2011,** *3*, 3962.